An Optimization Model for Resource Allocation in Multitenant LoRaWAN Scenarios

Natalia Chinchilla-Romero, Jonathan Prados-Garzon, Felix Delgado-Ferro, and Jorge Navarro-Ortiz

***Abstract*—Long Range Wide Area Network (LoRaWAN) has emerged as a leading Low Power Wide Area Network (LPWAN) solution for enabling connectivity in Internet of Things (IoT) wireless networks. The network slicing paradigm facilitates multitenancy and allows heterogeneous applications with diverse Quality of Service (QoS) requirements to coexist in various IoT use cases. This article addresses the radio resource allocation problem in a multitenant LoRaWAN network, where each tenant may serve multiple applications supported by Network Slicing (NS). To this end, we propose an optimization model to determine the optimal channel and Spreading Factor (SF) allocation for each end device in a multioperator environment with heterogeneous applications. The model maximizes aggregated normalized throughput while ensuring fairness among Network Operators (NOs), employing linearization strategies to solve the problem efficiently. Our evaluation demonstrates the maximum achievable LoRaWAN network capacity to accommodate diverse IoT smart city applications from different tenants. The results confirm that optimal resource allocations can be achieved within reasonable time frames while meeting all requirements, including fair resource distribution among slices, compliance with regulatory constraints, such as duty cycle limitations, assurance of QoS metrics (throughput, delay, and packet delivery ratio) for each NO, and full isolation of resources allocated to different NOs.**

***Index Terms*—Channel, Internet of Things (IoT), long range wide area network (LoRaWAN), multitenancy, network slicing (NS), optimization, resource allocation, spreading factor (SF).**

I. Introduction

THE NUMBER of connected devices in wireless networks has been experiencing significant growth in recent years. As a matter of fact, predictions forecast approximately 30 billion Internet of Things (IoT) connections by 2027, as stated in [1]. Most of these devices demand massive Machine Type Communication (mMTC) services, which is one of the three core Fifth Generation (5G) service categories. The applications covered by the mentioned mMTC 5G category range in a wide variety of services demanded by various different vertical business and use cases, such as smart cities, smart building, smart grid, logistics and agriculture, to name a few. In addition to the heterogeneity of Quality of Service (QoS) requisites required by all these applications, the IoT devices used in these long range scenarios must be low power consumers, cheap, and secured. In this vein, LPWANs play a significant role in the connection of IoT devices that are low power consumption, long range, low cost and secured [2].

In particular, all the mentioned features and requisites make Long Range Wide Area Network (LoRaWAN) be the most suitable wireless technology able to cover wide area scenarios and to serve a diverse variety of use cases in which other existing wireless technologies might not be the best to provide connectivity in a cost-effective way [3]. Additionally, the number of LoRaWAN deployments is increasing more rapidly compared to other IoT network solutions since it operates in the Industrial, Scientific and Medical (ISM) band and there is no need for a mobile operator to be involved, easing the deployment process. Nonetheless, meeting the QoS requirements of coexisting heterogeneous services demanded by different vertical businesses (e.g., smart building and smart grid) is a very challenging task. In this regard, multitenancy and Network Slicing (NS) are key enablers that arose with the advent of the 5G of mobile networks. On the one hand, multitenancy capability of 5G networks allows for serving multiple customers (namely tenants) over multiple instances of an application operating in a shared environment or infrastructure. Additionally, each tenant might be able to customize its application according to its business needs. On the other hand, NS emerges as a solution in 5G to simultaneously accommodate a wide range of services that vertical use cases will demand over a common network infrastructure. It enables the creation of end-to-end logical virtualized networks running on a common underlying network, mutually isolated with independent control and management with the aim of delivering customized solutions to meet the diverse QoS requirements in 5G multitenant networks [4]. So that, the network slicing paradigm might be able to handle differentiated network traffic according to the associated Service Level Agreements (SLAs) of each specific tenant.

However, realizing independent virtual mobile networks via network slicing in multitenancy requires efficient radio resource allocation and management to ensure the level of security and the QoS required by every network slice. This is even a more challenging task in LoRaWAN in which several difficulties lie ahead.

1) Radio resources are scarce and limited.
2) The operation band of LoRaWAN has several restrictions depending on the regulatory regions of the world [5]. For instance, in Europe a duty cycle limitation is imposed. Moreover, there is a maximum application

Received 10 January 2025; revised 4 April 2025; accepted 6 May 2025. Date of publication 12 May 2025; date of current version 25 July 2025. *(Corresponding author: Natalia Chinchilla-Romero.)*

The authors are with the Department of Signal Theory, Telematics and Communications and the Research Center on Information and Communication Technologies, University of Granada, 18014 Granada, Spain (e-mail: nataliachr@ugr.es; jpg@ugr.es; felixdelgado@ugr.es; jorgenavarro@ugr.es).

Digital Object Identifier 10.1109/JIOT.2025.3569060

© 2025 The Authors. This work is licensed under a Creative Commons Attribution 4.0 License.
For more information, see https://creativecommons.org/licenses/by/4.0/

payload limitation (up to 250 bytes) depending on the Data Rate (DR) used on its physical layer Long Range (LoRa) [6].

3) ALOHA is the protocol used to access the channel [7].

All these challenges lead us to propose a radio resource allocation optimization problem in a multitenant LoRaWAN network.

In this vein, the main objective of this work is to model the resource allocation problem in multitenant LoRaWAN networks and solve it efficiently using exact optimization methods. More precisely, we consider a scenario in which a LoRaWAN network is shared among multiple tenants, each managing diverse IoT applications, leveraging network slicing to ensure isolation and fairness in resource allocation among the tenants.

To that end, we formally formulate a novel optimization problem designed to determine the allocation of channels and SFs for end-devices (EDs) that maximizes the aggregated throughput of the system and the fairness among the Network Operators (NOs) (tenants) sharing the LoRaWAN infrastructure. The proposed model accounts for diverse application requirements and QoS treatment differentiation among NOs (e.g., minimum throughput, maximum delay and minimum packet delivery ratio), regulatory and tenant-specific constraints, and the operation of LoRa radio technology. Furthermore, the model is agnostic to the environmental radio conditions and the spatial distribution of the end devices. To improve computational efficiency, linearization techniques are employed. We then assess the maximum achievable capacity of a LoRaWAN network in supporting a representative range of smart city IoT applications from different tenants. Our findings highlight the feasibility of achieving optimal resource allocations within a reasonable time frame, ensuring fairness across slices, maintaining a minimum success probability for each LoRa Resource Block (RB), and providing complete isolation of resources among network operators.

Last, it should be noted that although this work assumes static input parameters, the proposed resource allocation model can be adapted to dynamic scenarios by periodically recalculating the configuration as environmental conditions change. The feasibility of this approach depends on the rate of significant changes in the input parameters, the available computational resources for solving the problem, and the execution environment (e.g., virtualization, operating system, programming language). In addition, reactive solutions can complement this process by allowing rapid adjustments between recalculations to address unexpected changes effectively.

The rest of the article is organized as follows. Section II gives a brief overview of the related existing works, highlighting the added value of this work compared to them. Section III includes the abstract model of the system and primary premises considered in this work. Section IV provides the problem statement (in Section IV-A), its formal formulation (in Section IV-B), and its linearization (in Section IV-C) in order to be solved efficiently. The experimental setup and results are reported and discussed in Section V. Last, Section VI includes the future work and concludes the article.

II. Related Works

The application of the NS paradigm over LoRa networks has gained momentum in recent years. NS over LoRaWAN is being studied to provide solutions that ensure QoS satisfaction and isolation among multiple services or tenants sharing the same physical LoRa network infrastructure. In this regard, several resource allocation solutions applying NS in LoRaWAN have been investigated over the years.

References [8], [9], [10], [11], [12], [13], and [14] propose centralized and distributed channel reservation, Transmission Power (TP), and Spreading Factor (SF) dynamic assignment solutions within an Software Define Network (SDN)-based architecture. They define three slices with different QoS requirements in terms of delay, urgency, and Packet Error Rate (PER). The device admission to slices and the channel reservation for each slice are addressed using clustering algorithms, such as Balanced Iterative Reducing and Clustering method using Hierarchies (BIRCH) or Online Gaussian Mixture Model clustering (OGMM) for admission and Maximum Likelihood Estimation (MLE) estimations or Mini-Batch Gradient Descent (MBGD) for channel reservation.

In all these works, LoRa servers act as centralized entities responsible for assigning the appropriate slice to each device and determining the gateway that will transmit each LoRa packet. The assignment of TP and SF configurations for devices within slices (intraslicing configuration) relies on Analytical and Hierarchy Process (AHP), Geometric Mean Method (GMM), and Technique for Order of Preference by Similarity to Ideal Solution (TOPSIS) methods, aiming to maximize QoS while minimizing energy consumption and reliability costs.

In [12], a distributed solution is proposed. Admission to slices and interslicing assignments are performed by the gateways in the NS-LoRa network using coalitional game theory. Furthermore, [14] proposes a Federated Deep-Q Learning solution, where each gateway acts as an agent performing local resource allocation based on a Deep Q-Learning model for slice TP and SF configurations. These agents interact with a Deep Federated Global Model to meet dynamic slice QoS requirements.

Expanding on this, the study [15] introduces a heuristic-based admission control mechanism that allocates IoT devices to network slices according to service priority. Additionally, it incorporates Deep Federated Q-Learning (DFQL) to dynamically manage resources, such as SF and TP, based on the QoS demands of slice users.

Building upon the ideas presented in the aforementioned studies on the application of network slicing to differentiate various service requirements, Mardi et al. [16] and [17] proposed a heuristic deep Q-learning solution and three novel approaches based on Multi-Armed Bandit (MAB) algorithms, respectively. These methods aim to address resource allocation in LoRaWAN with the goal of maximizing the Packet Delivery Rate (PDR) while ensuring compliance with the SLA for each service. Moreover, in [18] it is proposed a clustering framework comprising three different types of clusters according to end-devices' applications and thus, different demands of QoS

in terms of guaranteed PDR on each cluster. They optimize the channel and SF selection by providing two resource allocation algorithms: 1) MixRA-opt, a Mixed-Integer Non Linear Program (MINLP) optimization-based approach and 2) MixRA-H, a heuristic approximation.

Additionally, [19] proposes a lightweight slicing approach, fully compatible with LoRaWAN specifications, to achieve traffic isolation (e.g., between confirmed, normal, and unsolicited traffic) and protection.

In parallel, SF and channel assignment in multioperator LoRaWAN deployments have been addressed in [20] and [21]. Fawaz et al. [20] proposed an optimization problem for proportional fair SF assignment. They first introduce a partial interoperator cooperation scheme, where the optimization problem is solved iteratively using a gradient ascent algorithm for the different networks. In this scheme, each network shares traffic generated by other co-located operators through a federated technology employing secure aggregation. Additionally, they propose an alternative algorithm based on noncooperative game theory, where each operator (player) seeks to maximize its throughput independently.

This work is extended in [21], where the authors propose a learning-based approach for scenarios with minimal or no cooperation between operators. In this approach, each operator uses Recurrent Neural Network (RNN)s, such as Long Short Term Memory (LSTM), to estimate the total packet delivery ratio and optimize its resource allocation accordingly.

Similarly, Bankov et al. [22] developd a heuristic Modulation and Coding Scheme (MCS) allocation algorithm tailored to heterogeneous LoRaWAN scenarios. This algorithm considers different groups of EDs, each with distinct QoS requirements and varying traffic intensities. By employing a mathematical model to calculate the Packet Lost Ratio (PLR) distribution for the EDs, the authors use a heuristic algorithm to assign the MCS effectively.

Table I presents a comprehensive comparison of existing studies and ours, emphasizing key aspects, such as support for slicing, multitenancy and service heterogeneity, as well as the mechanisms used to ensure isolation among different slices (see columns 2, 3, 4, and 5). It should be noted that "N/A" is used to denote cases where a particular feature is not applicable. Slicing support refers to whether the work considers the potential division of the physical network into multiple customized virtual networks, known as network slices. Conversely, multitenancy support indicates whether the work includes mechanisms to facilitate and enhance the shared use of the LoRaWAN network by multiple tenants. Finally, service heterogeneity refers to the number of Types of Service (ToS), defined by their performance metrics, that can be distinguished by the proposed solution, as well as the approach used to meet the performance requirements of each ToS. Specifically, distinct perceived performance for each service can be achieved through mechanisms, such as prioritizing traffic over others (labeled as "priority" in column 5), selecting specific SFs for a type of traffic (labeled as "SF" in column 5)—e.g., SF 7 is appropriate for traffic with stricter latency requirements—or varying the load on a specific RB (labeled as "load" in column 5).

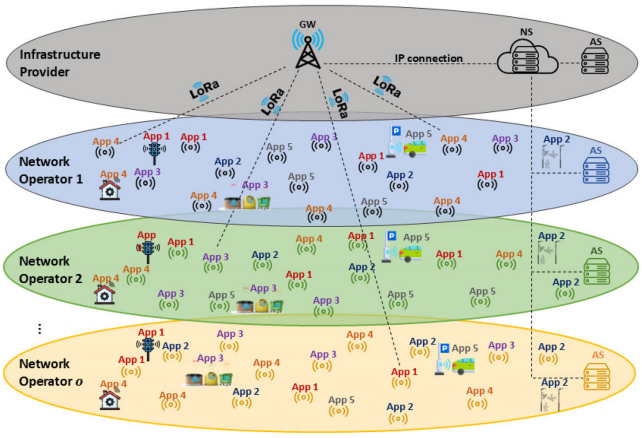


Fig. 1. System model.

The table also includes key performance requirements (see column 6), with a tick mark indicating whether a study guarantees specific metrics: throughput (T), delay (D), and packet success rate (P). It should be noted that studies addressing delay guarantees refer specifically to transmission delay, also known as Time on Air (ToA), which depends on the SF. It is important to clarify LoRaWAN's ability to provide delay guarantees. Specifically, it is possible to guarantee transmission delay (considering only the physical layer) or an average delay when considering the link layer. However, it cannot provide bounds for maximum delay under any circumstances.

Lastly, the optimization objectives addressed in each study, along with the methodologies employed by the proposed solutions, are presented in columns 6 and 7 of Table I.

To the best of our knowledge, this is the first work to propose a LoRaWAN radio resource allocation framework with multitenancy support, QoS differentiation in terms of throughput, delay, and PDR, and full performance isolation among NOs. Additionally, maximizing fairness among NOs, which has received little attention in the literature, is addressed for the first time. This innovative framework tackles practical challenges by incorporating service heterogeneity with varying QoS requirements, ensuring adaptability to scenarios with diverse and heterogeneous traffic patterns. It is particularly well-suited to environments featuring multiple tenants and distinct ToSs, where performance guarantees and fair allocation are essential. It is also noteworthy that the LoRaWAN operational specificities and regulatory constraints are fully respected, making our proposal fully compliant with the standards.

III. System Model

This section presents the abstract model for LoRaWAN, focusing on the network architecture, radio resource management, traffic patterns, and LoRa radio technology. The model establishes the assumptions and parameters that guide the resource allocation proposal in Section IV.

A. LoRaWAN Network Architecture

Let us consider a LoRaWAN network operated by an Infrastructure Provider (InP) consisting of end-devices (EDs), a gateway (GW) and a network server [29]. EDs, also

TABLE I
EXISTING WORKS COMPARISON

Work	Slicing Support	Isolation	Multi-tenancy Support	Service Heterogeneity	Perf. Reqs.			Target Goals	Methodology
					T	D	P		
[8]	Yes	Channel-based	No	3 ToS / priority	✓	✓	✓	Maximize customized utility function that depends on reliability energy consumption and number of accommodated EDs	1) BIRCH for EDs' admission to slices 2) MLE-based inter-slicing algorithm 3) AHP-based intra-slicing algorithm
[9]	Yes	Channel-based	No	3 ToS / priority	✓	✓	✓	Maximize QoS requirements and reliability, and minimize energy consumption to find the best SF and TP configuration	GMM and TOPSIS algorithms
[10]	Yes	Channel-based	No	3 ToS / priority	✓	✓	✓	Similar to the approach in [8], but with added adaptivity	1) BIRCH for EDs' admission to slices 2) Dynamic MLE-based inter-slicing algorithm 3) AHP-based intra-slicing algorithm
[12]	Yes	Channel-based	No	3 ToS / priority	✓	✓	✓	Similar to the approach in [8], but using a distributed approach	Coalitional and One-to-one matching game theory
[13]	Yes	Channel-based	No	3 ToS / priority	✓	✓	✓	Customized probability cost function that minimizes energy consumption and maximizes QoS	1) OGMM for EDs' admission to slices 2) MBGD for dynamic resource reservation 3) Max-Utility Inter-slicing algorithm
[11]	Yes	Channel-based	No	3 ToS / priority	✓	✓	✓	Similar to the approach in [9], but with added adaptivity	1) MLE to estimate slice members throughput 2) GMM to define objectives importance for each slice 3) TOPSIS to find the solution that maximizes utility requirements of slice members
[14]	Yes	Channel-based	No	3 ToS / priority	✓	✓	✓	Similar to [8], but including the maximization of total communication rate within an unit energy	Deep Reinforcement Learning (DRL)
[23]	Yes	Channel-based	No	3 ToS / priority	✓	✓	✓	Similar to [9]	DRL
[16]	Yes	Time and channel-based	No	3 ToS / priority	✓	✗	✓	Maximize services' PDR while ensuring prioritization between them	DRL and Heuristics
[17]	Yes	Time and channel-based	No	3 ToS / priority	✓	✗	✓	Maximize services' PDR while ensuring prioritization between them	MAB
[21]	No	Channel-based	Yes	N/A	✓	✗	✓	Maximize the total normalized throughput across all SFs and channels	Game Theory
[24]	No	Channel-based	Yes	N/A	✓	✗	✓	Similar to [21]	Game Theory
[20]	No	SF-based	Yes	N/A	✓	✗	✓	Maximize the total normalized throughput across all SFs	1^{st} method: Gradient-Ascent algorithm 2^{nd} method: Game Theory 3^{rd} method: LSTM
[25]	No	Hard and soft channel-based	No	3 ToS / load	✓	✗	✓	No objective. Finding feasible solution s.t. PDR requirements	Heuristics
[26]	No	Channel-based	No	3 ToS / load	✓	✗	✓	Maximize PDR in every ToS	COIN-OR Branch and Cut (CBC) solver
[27]	Yes	Channel-based	No	2 ToS / priority	✓	✗	✓	Maximize target PDR	Genetic Algorithm
[28]	Yes	Channel-based	No	3 ToS / priority	✓	✓	✓	Similar to [9]	Multi-agent Transfer Reinforcement Learning
[19]	Yes	SF-based	No	Arbitrary ToS / SF	✓	✗	✓	Finding feasible solution s.t. QoS requirements	Heuristics
[18]	No	Channel and SF based	No	3 ToS/ priority	✓	✗	✓	Maximize total network throughput	MINLP solver and heuristics
[15]	Yes	Channel-based	No	5 ToS / load	✓	✓	✓	Maximize slice's throughput and PDR. Minimize slice´s delay and energy consumption	DFQL
Ours	Yes	Channel and SF-based	Yes	Arbitrary ToS / load	✓	✓	✓	Maximize overall throughput and throughput fairness among tenants	MILP solver

commonly known as motes, are equipped with sensors or actuators, communicate wirelessly with GWs using LoRa radio technology. The communication between EDs and GWs can be two-way: 1) from EDs to GWs (uplink) and 2) from GWs to EDs (downlink). In the uplink, the network server collects messages from all GWs, eliminates duplicates, and forwards the messages to the appropriate Application Server (AS). In the downlink, the network server collects messages from ASs and selects the most suitable GW for transmission. The AS provides the service logic for the IoT application, such as processing sensed data.

The InP utilizes an infrastructure Network Slicing (NS) to enable multitenancy, facilitating the sharing of network infrastructure among a set of NOs $\in \mathcal{O} = o_1, o_2, \ldots, o_O$, as depicted in Fig. 1. Each NO serves IoT applications with diverse demand and QoS requirements. Specifically, each NO o manages N_o EDs or LoRaWAN EDs, each might be dedicated to a different IoT application. This work adopts an infrastructure NS approach similar to those proposed in [30], [31] for 5G private networks, where dedicated and well-isolated resources, managed by the InP, are provisioned for each infrastructure slice across all network domains. This ensures performance isolation among coexisting infrastructure slices.

In this study, we focus on the slicing of radio resources among the NOs, while assuming complementary algorithms manage resource distribution in the backhaul network (interconnecting the GWs with the network servers) and in the computing domain (hosting network servers and ASs). We consider the network server as the primary entity responsible for radio resource allocation, although it does not preclude the GWs and EDs may complement this process with local and more specific adjustments. This approach is widely adopted because the network server has comprehensive visibility into the connections between EDs and GWs, radio quality metrics (e.g., per-ED Signal-to-Noise Ratio (SNR)), and traffic patterns, enabling globally optimized allocation decisions. In addition, in many IoT scenarios, GWs lack the computational capacity required to execute the resource allocation algorithms. While the server could also manage the transmission power of each ED, this feature is not addressed in our work.

Having established the network architecture, we now describe the traffic patterns generated by EDs, which are crucial to establishing the resource allocation model.

TABLE II
GATEWAY SENSITIVITY FOR EACH SF

SF	s	Gateway Sensitivity (dBm)
12	6	-142.5
11	5	-140
10	4	-137.5
9	3	-135
8	2	-132.5
7	1	-130

B. ED Model

The EDs act as traffic sources in uplink and are arbitrarily distributed over the GW coverage area. As in many previous studies, we implicitly assume that the interpacket generation time for each ED follows an exponential distribution. The traffic demand of each ED i is characterized by its packet rate $\lambda_i^{(o)}$ and packet payload $L_i^{(o)}$. The packet rate $\lambda_i^{(o)}$ represents the average number of packets generated per unit time by ED i and is determined by the update time of the associated IoT application. Some IoT applications generate packets periodically (constant update time), while others produce event-based messages triggered by specific events, such as the temperature exceeding a given threshold. On the other hand, the packet payload $L_i^{(o)}$ refers to its total number of bits comprising the Medium Access Control (MAC) layer overheads and the useful information.

C. LoRa Radio Technology

1) LoRa Spectrum: LoRa radio technology uses the unlicensed ISM radio band. Unlicensed frequencies can be used by anyone and are free of charge. Regulatory bodies often impose restrictions or rules to manage spectrum usage and prevent network congestion, thus avoiding the band becomes unusable. Adhering to these rules helps ensure fair and efficient utilization of the available spectrum. Additionally, InPs and NOs might apply more restrictive rules for radio transmissions. These restrictions include the maximum transmission power, maximum antenna gain, maximum duty cycle d_c per ED for channel c, and maximum dwell time per ED. In particular, the duty cycle and dwell time are related to the channel occupation. On the one hand, duty cycle refers to the ratio of time the channel is busy versus the total observation time. On the other hand, dwell time refers to the amount of time that an ED spends on a specific channel before switching to the next channel. For instance, European Telecommunications Standards Institute (ETSI) recommends a maximum duty cycle of 0.1% for subband M (868–868.6 MHz) per ED, which translates into each ED can be active (transmitting) 86 s at most per day. The Things Network's fair access policy further limits the uplink airtime to 30 s per day per node [32].

2) Radio Resources: The available bandwidth is split into C orthogonal channels, each with bandwidth BW, and S SFs that can be used simultaneously over each channel [7], [33]. A pair consisting of a channel c and a SF s is referred to as a Resource Block (RB). SFs determine the modulation and coding scheme for data transmission. They represent different levels of spreading, affecting signal duration and robustness. Higher SFs result in longer spreading sequences, providing increased resistance to interference but also leading to longer transmission times. Conversely, lower SFs allow for faster data transmission with reduced robustness.

The use of a specific SF s is subject to the condition that the signal reaches the receiver with a minimum level of SNR $\mathrm{SNR}_s^{(\min)}$. Specifically, it holds that $\mathrm{SNR}_s^{(\min)} = -7.5\,\mathrm{dB} - 2.5 \cdot (s-7)\,\mathrm{dB}$. Otherwise, the receiver will not be able to properly demodulate the signal. These limits can be translated into the Received Signal Strength Indicator (RSSI) levels, γ_s, expressed in *dBm*, for each SF s using the following expression:

$$\gamma_s = -174\,\mathrm{dBm} + 10 \cdot \log_{10}(\mathrm{BW}) + \mathrm{NF} + \mathrm{SNR}_s^{(\min)} \quad (1)$$

where NF is the receiver noise figure specific to each LoRa hardware implementation. Observe that the weaker the signal is (e.g., due to a longer distance between the ED and the GW), the higher the SF is needed in order to lower the receiver sensitivity. The limit values of the RSSI levels for each SF are shown in Table II.

3) Packet Transmission Delay: The ToA, or total air transmission time, is the duration it takes for the radio transmission of a LoRa message to complete. The ToA is a critical parameter as it influences the maximum spectrum utilization, comply with regulatory duty cycle limitations, and EDs' energy consumption. Considering the explicit header mode (LoRaWAN default configuration [34]), the ToA $T_{i,s}^{(o)}$ for the packets generated by ED i from NO o using SF s is given by

$$T_{i,s}^{(o)} = \frac{2^s}{BW} \cdot \left((n_p + 4.25) + 8 + \max\left\{ \left\lceil \frac{\left(L_i^{(o)} - 4 \cdot s + 28 + 16\right)}{4 \cdot (s - 2 \cdot \mathrm{LDR})} \right\rceil \cdot (CR + 4), 0 \right\} \right) \quad (2)$$

where n_p is the number of symbols in the packet preamble (e.g., eight symbols for EU868 frequency band), $CR \in \{1, 2, 3, 4\}$ determines the coding rate, and LDR is a binary variable indicating whether the Low Data Rate Optimization (LDRO) is enabled (LDR = 1) or not (LDR = 0). LDRO involves adaptive strategies and protocol adjustments to improve reliability when EDs operate at lower data rates.

4) Medium Access Control: LoRa radio technology utilizes ALOHA as the default medium access mechanism [33], allowing EDs to transmit data without first sensing the medium. This approach is favored for its simplicity, low complexity, and the autonomy it provides to EDs. However, the absence of medium sensing leads to collisions, which occur when two or more EDs transmit simultaneously on the same resource block. This results in interference, often corrupting the transmitted packets and rendering them uninterpretable by the GW.

The capture effect mitigates collision impacts by allowing a gateway to decode a packet when its signal strength sufficiently exceeds interfering signals (e.g., by 6 dB) [29]. However, this study deliberately excludes it, aligning with most prior work (see Section II, "Related Works"), to maintain a conservative baseline. While incorporating the capture effect introduces a positive bias to the per-RB throughput function [35], [36], reflecting enhanced performance, its exclusion ensures a focus on worst-case scenarios. By adopting this conservative model, the proposed resource allocation is

expected to reliably meet minimum throughput requirements in real-world LoRaWAN deployments.

D. Radio Resource Allocation

The radio resource allocation process takes several input parameters, including SNR metrics, EDs traffic characteristics, the mapping of EDs to NOs, and the performance requirements of each NO. Based on these inputs, it outputs the radio configuration for each ED, ensuring compliance with all relevant constraints, such as regulatory limitations and performance requirements. This approach is deployment-agnostic and can be applied in various scenarios (e.g., urban, suburban or rural). Notably, we do not make assumptions about signal propagation or interference; instead, per-ED SNR is directly measured and used as an input for the radio resource allocation algorithm. For instance, in the experimental setup of this work, we evaluate the solution in a smart city environment within an urban area. However, the proposed approach is versatile and can be applied to other types of environments as well.

This work does not explicitly address dynamic resource provisioning, as it assumes that input parameters remain constant over time (e.g., due to EDs mobility). However, the proposed resource allocation model can be adapted for dynamic scenarios where environmental conditions change over time. This adaptation can be achieved by periodically solving the model and updating the resource allocation configuration accordingly. The frequency of solving the problem depends on the rate of significant changes in the input parameters, i.e., how often such changes call for recalculating the resource allocation configuration. The feasibility of this approach is also contingent on the computational resources available for solving the problem and the execution environment (e.g., whether it is a virtualized environment, the operating system, or the programming language used). Additionally, reactive solutions could complement this process by enabling rapid adjustments between periodic recalculations, thereby addressing unexpected changes promptly and effectively.

IV. Multitenant LoRa Radio Resource Allocation Proposal

In this section, we address the radio resource allocation problem in a multitenancy LoRaWAN for uplink transmissions.

A. Problem Statement

In the context of a LoRaWAN GW managed by an InP and multiple NOs (considered each as a network slice) sharing the infrastructure, where each NO serves a set of EDs (N_o) associated with heterogeneous smart city IoT applications, the objective is to allocate a set of radio resources to each NO for uplink transmissions. This allocation aims to maximize the offered throughput of the GW as well as fairness among the NOs. Specifically, an RB, defined as a pair of LoRa channel and SF, is allocated to each ED if possible. It could happen there is not a feasible resource allocation for all the EDs given the constraints of the problem. In such case, an allocation maximizing fairness among NOs is preferred. In particular, the throughput deficit for every NO, i.e., difference between the aggregated demanded throughput and offered throughput, must be as similar as possible. The problem is governed by the following requirements.

1) Ensuring the allocated RB to each ED is enough as to meet its throughput demand.
2) Allocating segregated RBs to each NO for isolation. In this way, if an ED from NO $o \in \mathcal{O}$ generates nonconformant traffic, it will only negatively affect other EDs served by the same NO. Therefore, it is ensured that the traffic excess generated by the EDs from a given NO will not degrade the performance perceived by the rest of NOs.
3) Warranting a maximum probability of collision and maximum delay per NO during the transmissions through every channel-SF pair.
4) Meeting the regulatory constraints imposed by either the regulatory authorities, InP or NO. These stakeholders might impose restrictions on radio transmissions, as mentioned in the previous section. Taking them into account is a must to compute feasible real-world resource allocations.
5) Assuring the minimum SNR level to properly demodulate the uplink signal of each ED at the GW.

B. Problem Formulation

Building upon the system model described in the preceding section, the formal formulation of the LoRaWAN resource allocation problem addressed in this work is provided next. We formulate the resource allocation problem as a multiobjective optimization program that maximizes the overall throughput of the system and equalizes the throughput deficits among the NOs. The optimization program's output is the mapping of EDs onto RBs. One RB might serve multiple EDs from the same NO. To that end, we define the decision binary variables $U_{i,c}^{(o)}$ and $V_{i,s}^{(o)}$ that, respectively, indicate whether the ED i from NO o is allocated to channel c and SF s ($U_{i,c}^{(o)} \cdot V_{i,s}^{(o)} = 1$) or not. Table III includes the primary notation used in the problem formulation.

$$\text{maximize} \left\{ \sum_{c=1}^{C} \sum_{s=1}^{S} G_{s,c} \cdot \exp\left(-2G_{s,c}\right) \right\} \tag{3}$$

$$\text{minimize} \left\{ \sum_{o=1}^{O} |\Lambda \cdot \Phi_o - \Lambda_o \cdot \Phi| \right\} \tag{4}$$

where

$$\Lambda_o = \sum_{i=1}^{N_o} \lambda_i^{(o)} \cdot I\left(P_i^{(o)} \geq \gamma_S\right) \tag{5}$$

$$\Lambda = \sum_{o=1}^{O} \Lambda_o \tag{6}$$

s.t.

$$G_{s,c} = \sum_{o=1}^{O} \sum_{i=1}^{N_o} U_{i,c}^{(o)} \cdot V_{i,s}^{(o)} \cdot \lambda_i^{(o)} \cdot T_{i,s}^{(o)} \quad \forall\, c \in [1, C];\ s \in [1, S] \tag{7}$$

$$\Phi_o = \sum_{i=1}^{N_o} \sum_{c=1}^{C} \sum_{s=1}^{S} U_{i,c}^{(o)} \cdot V_{i,s}^{(o)} \cdot \lambda_i^{(o)} \quad \forall\, o \in [1, O] \tag{8}$$

$$\Phi = \sum_{o=1}^{O} \Phi_o \tag{9}$$

$$\lambda_i^{(o)} \cdot \sum_{s=1}^{S} V_{i,s}^{(o)} \cdot T_{i,s}^{(o)} \leq \sum_{c=1}^{C} U_{i,c}^{(o)} \cdot d_c \quad \forall o \in [i, O], i \in [1, N_o] \tag{10}$$

$$\exp(-2 \cdot G_{s,c}) \geq \max_{\forall o \in [1,O]} \left\{ I\left(N_{s,c}^{(o)} \geq 1\right) \cdot Q^{(o)} \right\} \quad \forall s \in [1, S];\ c \in [1, C] \tag{11}$$

$$V_{i,s}^{(o)} \leq I\left(T_{\max}^{(o)} \geq T_{i,s}^{(o)}\right) \quad \forall s \in [1, S];\ o \in [1, O];\ i \in [1, N_o] \tag{12}$$

$$\left(\sum_{i=1}^{N_{o_1}} U_{i,c}^{(o_1)} \cdot V_{i,s}^{(o_1)}\right) \cdot \left(\sum_{i=1}^{N_{o_2}} U_{i,c}^{(o_2)} \cdot V_{i,s}^{(o_2)}\right) \leq 0 \quad \forall c \in [1, C];\ s \in [1, S];\ o_1, o_2 \in [1, O]\ \ s.t.\ o_1 \neq o_2 \tag{13}$$

$$V_{i,s}^{(o)} \leq I\left(P_i^{(o)} \geq \gamma_s\right) \forall s \in [1, S];\ o \in [1, O];\ i \in [1, N_o] \tag{14}$$

$$\sum_{c \in C} U_{i,c} \leq 1 \quad \forall o \in [1, O];\ i \in [1, N_o] \tag{15}$$

$$\sum_{s \in S} V_{i,s} \leq 1 \quad \forall o \in [1, O];\ i \in [1, N_o]. \tag{16}$$

The primary objective of optimization (3) is to maximize the aggregated uplink goodput of the GW. Throughput calculations are based on the methodology proposed in [21], which involves summing the data generated by each ED and multiplying it by the transmission time or ToA of the corresponding packet. In parallel, objective (4) aims to align the offered throughput with the demanded throughput for every NO whenever possible. In cases where this alignment is not feasible, the objective strives to equalize the throughput deficit among NOs, promoting fairness among them.

Equations (5)–(9) introduce auxiliary variables. Γ_o denotes the aggregated throughput demanded by NO o, while Γ represents the total aggregated throughput demanded by all NOs. Additionally, $G_{s,c}$ represents the offered throughput of the RB, which is defined as a pair of LoRa radio channel c and a SF s. The variables G_o and G denote the aggregated offered throughput of NO o and the GW, respectively. These variables, namely, $G_{s,c}$, G_o, and G, are introduced as auxiliary decision variables to reduce the implementation complexity of the program.

Concerning the inequality constraints, (10) ensures that each end device complies with duty cycle limitations set by regulatory bodies, InPs, and Network Operators (NOs). For instance, ETSI provides corresponding recommendations [5], adopted by local regulatory authorities in various countries, including European nations and China.

Constraints (11) and (12) ensure that the performance requirements in terms of PDR and latency are met, enabling differentiation among NOs. The binary function $I(l)$ evaluates to 0 if the logical condition l is not satisfied and 1 otherwise. $N_{s,c}^{(o)}$ represents the number of EDs from NO o allocated to channel c and SF s. $Q^{(o)}$ and $T_{\max}^{(o)}$ denote the most restrictive QoS requirement among the maximum PLR and maximum delay that must be satisfied, and the target maximum delay, respectively.

Under the assumption that LoRaWAN confirmed traffic is used for a given NO o, the problem input parameter $Q^{(o)}$ is set to:

$$Q^o = \max\left\{ \frac{T_{i,s}^{(o)} + D}{T_{\max}^{(o)} - T_{i,s}^{(o)} - D}, \left(1 - P_{c,\max}^{(o)}\right) \right\} \tag{17}$$

where D is the mean backoff retransmission time after a collision, and $P_{c,\max}^{(o)}$ is the target maximum probability of collision for NO o. In this way, both a maximum mean delay and maximum probability of collision are ensured.

For unconfirmed traffic, there are no retransmissions and delay is only given by the ToA, which is warranted by constraints (12). Thus, $Q^{(o)}$ must be directly set to

$$Q^o = 1 - P_{c,\max}^{(o)}. \tag{18}$$

Constraints (13) establish isolation between NOs, allocating each RB to end devices served by the same NO.

Constraints (14) restrict the SFs that can be allocated to each end device to ensure that the minimum SNR level is reached at the GW for proper signal demodulation. Specifically, the allocation of a given SF to an end device i is subject to the received power $P_i^{(o)}$ at the GW being greater than or equal to its sensitivity γ_s (e.g., γ_1 represents the GW sensitivity for SF 7). As indicated in (1), γ_s decreases for higher SFs. In (14), $I(l)$ denotes a binary function that outputs 0 if the logical condition l is not met, or 1 otherwise.

Finally, constraints (15) and (16) enforce that only one RB is allocated to each end device.

It can be formally proven that the problem described above is NP-hard, as demonstrated in the Appendix of this article.

TABLE III
PRIMARY NOTATION

Notation	Description
$\mathcal{O}$	Set of NOs with cardinality $O = \lvert\mathcal{O}\rvert$.
C	Number of orthogonal radio channels.
S	Number of available SFs.
N_o	Number of EDs from operator $o \in \mathcal{O}$.
BW	Channel bandwidth.
$U_{i,c}^{(o)}$	Decision binary variable indicating whether the channel $c \in \mathcal{C}$ is allocated to the ED i from NO o ($U_{i,c}^{(o)} = 1$) or not ($U_{i,c}^{(o)} = 0$).
$V_{i,s}^{(o)}$	Decision binary variable indicating whether the SF s is allocated to the ED i from NO o ($V_{i,s}^{(o)} = 1$) or not ($V_{i,s}^{(o)} = 0$).
$\lambda_i^{(o)}$	Packet generation rate for ED i from NO o.
Λ_o	Aggregate offered (demanded) traffic rate from NO o.
Λ	Aggregate offered (demanded) traffic rate by all the NOs.
$G_{s,c}$	Traffic intensity allocated to channel c and SF s pair.
Φ_o	Aggregate carried traffic rate in the system from NO o.
Φ	Aggregate carried traffic rate in the system from all the NOs.
d_c	Maximum duty cycle per device for channel c.
γ_s	LoRa receiver sensitivity for SF s.
$T_{i,s}^{(o)}$	Average ToA for the ED i from NO o when it uses SF s.
$P_{c,max}^{(o)}$	Maximum collision probability for NO o.
$P_i^{(o)}$	Received power at the GW from ED i from NO o.
$Q^{(o)}$	Model input parameter accounting for both PLR and delay requirements for NO o.
$T_{max}^{(o)}$	Target maximum delay for NO o.
D	Mean backoff retransmission time after a collision.

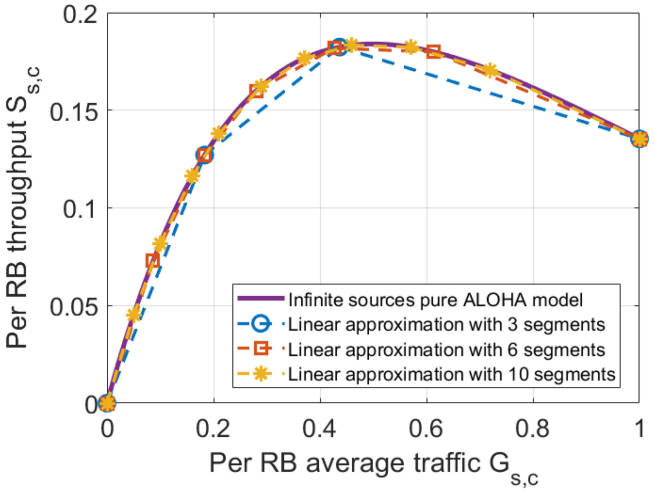


Fig. 2. Piecewise linear approximations considering different number of segments for the infinite sources pure ALOHA model.

C. Problem Linearization

This section focuses on linearizing the problem defined in (3)–(16). The optimization objectives (3) and (4), along with constraints (7), (8), (11), and (13), are inherently nonlinear. The purpose of this linearization is to efficiently solve tractable instances of the problem.

First, we linearize the optimization goal (3). For each RB defined by the SF s and channel c, the interval of interest for $G_{s,c}$, i.e., $0 \leq G_{s,c} \leq G_{s,c}^{(\max)}$, is divided into N sampling points or breakpoints: $G_{s,c}^{(1)} = 0, G_{s,c}^{(2)}, \ldots, G_{s,c}^{(N)} = G_{s,c}^{(\max)}$. The sampling points can be chosen using an algorithm that minimizes the maximum absolute error between the original function and its piecewise linear approximation, achieving a balance between accuracy and computational efficiency, as described in [37]. The value of $G_{s,c}^{(N)} = G_{s,c}^{(\max)}$ is determined based on the target collision probability by solving $\exp(-2 \cdot G_{s,c}^{(N)}) = (1 - P_c^{(\max)})$, as the maximum traffic intensity accommodated by an RB must adhere to constraint (11).

Given these sampling points, the throughput $S_{s,c}(G_{s,c})$ is approximated by linear segments connecting consecutive points

$$\left\{\left(G_{s,c}^{(n)}, S_{s,c}\left(G_{s,c}^{(n)}\right)\right), \left(G_{s,c}^{(n+1)}, S_{s,c}\left(G_{s,c}^{(n+1)}\right)\right)\right\}. \quad \forall n \in [1, N-1].$$

This approximation is expressed as follows for each segment:

$$S_{s,c}(G_{s,c}) \approx S_{s,c}\left(G_{s,c}^{(n+1)}\right) - m_n \cdot \left(G_{s,c}^{(n+1)} - G_{s,c}\right)$$
$$G_{s,c}^{(n)} \leq G_{s,c} \leq G_{s,c}^{(n+1)} \tag{19}$$

where m_n is the slope of the segment n that is given by

$$m_n = \frac{S_{s,c}\left(G_{s,c}^{(n+1)}\right) - S_{s,c}\left(G_{s,c}^{(n)}\right)}{G_{s,c}^{(n+1)} - G_{s,c}^{(n)}}.$$

Now, we introduce auxiliary decision variables and constraints to combine the different segments and linearize the resulting piecewise linear approximation. Specifically, we define auxiliary binary variables $B_{s,c}^{(n)}$ and continuous variables $W_{s,c}^{(n)} \forall s \in [1, S]$, $c \in [1, C]$, $n \in [1, N-1]$ and add the following constraints:

$$\sum_{n=1}^{N-1} B_{s,c}^{(n)} = 1 \quad \forall s \in [1, S];\ c \in [1, C] \tag{20}$$

$$W_{s,c}^{(n)} \geq G_{s,c}^{(n)} \cdot B_{s,c}^{(n)} \quad \forall s \in [1, S];\ c \in [1, C];\ n \in [1, N-1] \tag{21}$$

$$W_{s,c}^{(n)} \leq G_{s,c}^{(n+1)} \cdot B_{s,c}^{(n)} \quad \forall s \in [1, S];\ c \in [1, C];\ n \in [1, N-1] \tag{22}$$

$$\sum_{n=1}^{N-1} W_{s,c}^{(n)} = G_{s,c}. \tag{23}$$

Then, (3) can be rewritten as

$$\text{minimize} \left\{ \sum_{c=1}^{C} \sum_{s=1}^{S} \sum_{n=1}^{N-1} -S_{s,c}\left(G_{s,c}^{(n+1)}\right) \cdot B_{s,c}^{(n)} + m_n \cdot G_{s,c}^{(n+1)} \cdot B_{s,c}^{(n)} - m_n \cdot W_{s,c} \right\}. \tag{24}$$

Fig. 2 compares the piecewise linear approximation for the normalized throughput of the infinite sources pure ALOHA model in (3) using different numbers of segments. Increasing the number of segments improves approximation accuracy at the cost of additional auxiliary decision variables and constraints. In Section V-B, we report the impact of the number of segments to approximate the per-RB throughput function on the computational complexity of solving the resulting optimization program.

Now, we can unify both objectives, labeled as (24) and (4), into a single expression using a convex sum, as shown below

$$\text{minimize} \left\{ \frac{\alpha}{C \cdot S} \cdot \sum_{c=1}^{C} \sum_{s=1}^{S} \sum_{n=1}^{N-1} \left(-S_{s,c}\left(G_{s,c}^{(n+1)}\right) \cdot B_{s,c}^{(n)} + m_n \cdot G_{s,c}^{(n+1)} \cdot B_{s,c}^{(n)} - m_n \cdot W_{s,c} \right) + \frac{\beta}{O \cdot \Lambda \cdot \overline{\Lambda}_o} \cdot \sum_{o=1}^{O} |\Lambda \cdot \Phi_o - \Lambda_o \cdot \Phi| \right\}. \tag{25}$$

Here, α and β represent two parameters of the problem, satisfying the constraint $\alpha + \beta = 1$. These parameters allow us to adjust the importance of objectives (24) and (4), respectively. To remove the absolute values in the equation above, we introduce auxiliary continuous variables $X_o = |\Lambda \cdot \Phi_o - \Lambda_o \cdot \Phi| \, \forall o \in [1, O]$. Then we can rewrite the optimization goal as below

$$\text{minimize} \left\{ \frac{\alpha}{C \cdot S} \cdot \sum_{c=1}^{C} \sum_{s=1}^{S} \sum_{n=1}^{N-1} \left(-S_{s,c}\left(G_{s,c}^{(n+1)}\right) \cdot B_{s,c}^{(n)} + m_n \cdot G_{s,c}^{(n+1)} \cdot B_{s,c}^{(n)} - m_n \cdot W_{s,c} \right) + \frac{\beta}{O \cdot \Lambda \cdot \overline{\Lambda}_o} \cdot \sum_{o=1}^{O} X_o \right\}. \tag{26}$$

To enforce the variables G_o take the desired value, we include

the following set of constraints:

$$X_o \geq \Lambda \cdot G_o - \Lambda_o \cdot G \quad \forall\, o \in [1, O] \tag{27}$$

$$X_o \geq -\Lambda \cdot G_o + \Lambda_o \cdot G \quad \forall\, o \in [1, O]. \tag{28}$$

To linearize the equality constraints (7) and (8), it is required to remove the product of the decision variables $U_{i,c}^{(o)}$ and $V_{i,s}^{(o)}$. This can be done by introducing a new set of auxiliary binary variables $\delta_{i,c,s}^{(o)} = U_{i,c}^{(o)} \cdot V_{i,s}^{(o)}$ and adding new constraints. Then, (7) and (8) become

$$G_{s,c} = \sum_{o=1}^{O} \sum_{i=1}^{N_o(O)} \delta_{i,c,s}^{(o)} \cdot \lambda_i^{(o)} \cdot T_{i,s}^{(o)} \quad \forall\, c \in [1, C];\ s \in [1, S] \tag{29}$$

$$G_o = \sum_{i=1}^{N_o} \sum_{c=1}^{C} \sum_{s=1}^{S} \delta_{i,c,s}^{(o)} \cdot \lambda_i^{(o)} \cdot T_{i,s}^{(o)} \quad \forall\, o \in [1, O]. \tag{30}$$

Besides, the new constraints to be added are the following:

$$\delta_{i,c,s}^{(o)} - U_{i,c}^{(o)} \leq 0 \quad \forall\, o \in [1, O];\ i \in [1, N_o];\ c \in [1, C] \tag{31}$$

$$\delta_{i,c,s}^{(o)} - V_{i,s}^{(o)} \leq 0 \quad \forall\, o \in [1, O];\ i \in [1, N_o];\ s \in [1, S] \tag{32}$$

$$U_{i,c}^{(o)} + V_{i,s}^{(o)} - \delta_{i,c,s}^{(o)} \leq 1 \quad \forall\, o \in [1, O];\ i \in [1, N_o];\ c \in [1, C];\ s \in [1, S]. \tag{33}$$

Regarding (13), we can linearize it by introducing the auxiliary binary variables $\Delta_{c,s}^{o} \forall\, c \in [1, C]$, $s \in [1, S]$ and $o \in [1, O]$ the following two additional constraints:

$$\sum_{o=1}^{O} \Delta_{c,s}^{o} \leq 1 \quad \forall\, c \in [1, C];\ s \in [1, S] \tag{34}$$

$$\sum_{i=1}^{N_o} \delta_{i,c,s} \leq N_o \cdot \Delta_{c,s}^{o} \quad \forall\, o \in [1, O];\ c \in [1, C];\ s \in [1, S]. \tag{35}$$

Finally, using $\Delta_{c,s}^{o} \forall\, c \in [1, C]$, $s \in [1, S]$, whose value is 1 if channel c and SF s are assigned to NO o, and taking the natural logarithm, constraints (11) can be linearized as

$$G_{s,c} \leq -\frac{1}{2} \cdot \sum_{o=1}^{O} \Delta_{c,s}^{o} \cdot \ln\left(Q^{(o)}\right) \quad \forall\, s \in [1, S];\ c \in [1, C]. \tag{36}$$

Then optimization problem with objective (26) subject to (20), (21), (22), (23), (27), (28), (29), (30), (9), (31), (32), (33), (10), (36), (12), (34), (35), (14), (15), and (16) is a Mixed-Integer Linear Program (MILP) equivalent to the original LoRaWAN radio resource allocation problem that can be solved more efficiently.

V. Results

With the aim of assessing the capacity of a LoRaWAN InP to do an efficient resource allocation of LoRa resources in the context of multitenant and heterogeneous LoRa networks, we carried out a simulation evaluation of the designed proposal formulated in Section IV-C. To this end, we implemented our mathematical model in MATLAB, using CVX (a disciplined convex optimization modeling language) and we solved it using the powerful optimizer Gurobi solver on a server with and Intel Core i9-10920X CPU @3.50 GHz, 256 GB of RAM in Windows 11 Pro operating system. Section V-A explains the experimental setup that we have followed to run the different simulations, Section V-B presents the results related to the algorithm's computational complexity, and Section V-C includes the main results extracted from the simulations, as well as a comprehensive analysis of them.

A. Experimental Setup

The experimental setup considered to perform different simulation evaluations is detailed hereunder. A LoRaWAN GW connected to a LoRaWAN network server belonging to an unique InP is deployed within a circular area of 5 Km in radius, as illustrated in Fig. 1. In this physical infrastructure, three slices belonging each to a different NO are deployed. All traffic generated by the EDs from the three NOs is unconfirmed, with a maximum collision probability requirement of 80% set for each. There is a total number of EDs in the network, which is fixed and distributed equally between the different NOs. These EDs are uniformly placed along the scenario and pertain to a different application within the smart city context. Specifically, the applications that have been considered are Heating, Ventilation, Air Conditioning (HVAC), Home Automation (HA), city lightning, waste management, and smart parking (see Table V). The applications' device density is derived from a real smart city architecture deployed in Barcelona city [38]. The specific values are included in the last column of Table V. Please, note that the percentage values specified in the table are referred to the total amount of end devices in the scenario.

EDs transmit periodical or event-based traffic with packet sizes of 10, 50, or 100 bytes contingent upon the specific application being executed. Considering the context of LoRaWAN smart city applications (both indoor and outdoor applications) [39], the packet size and the update time requirements have been collected from [2] and [40]. All the specific applications requirements are presented in Table V.

Furthermore, the received power at the GW side is determined using (37), where P_{TX} is the transmission power of the transmitter (ED), G_{TX} and G_{RX} represent the transmitter and the receiver antenna gains, respectively, and L_{OH} stands for the computed propagation losses. In this case, we have adopted the Okumura Hata path loss model, a widely well-known model for path loss estimation in LoRaWAN smart city scenarios [41]. With respect to (38), fc represents the carrier frequency, htx and hrx denote the respective transmitter and receiver antenna heights in meters, the parameter d_{tx-rx} signifies the spatial separation between the transmitter and receiver and a is the correction factor considering a small/medium urban area. Table IV provides a comprehensive listing of the transmission parameters, based on [6]

$$\begin{aligned} P_{RX}(dBm) &= P_{TX}(dBm) + G_{TX}(dBi) \\ &\quad + G_{RX}(dBi) - L_{OH}(\text{dB}) \\ L_{OH}(\text{dB}) &= 69.55 + 26.16 \cdot log_{10}(fc) - 13.82 \cdot log_{10}(h_{tx}) \end{aligned} \tag{37}$$

TABLE IV
TRANSMISSION PARAMETERS

Parameter	Value
Frequency channels	868.1, 868.3, 868.5 MHz
SFs	7,8,9,10,11,12
Bandwidth	125 kHz
Coding rate	4/5
Ptx	14 dBm
Gtx	2 dBi
Grx	2 dBi
htx	1.5 m
hrx	15 m
fc	868 MHz

TABLE V
APPLICATIONS REQUIREMENTS

Application	Packet Size	Update Time / Packet Rate	Device Density
HVAC	50-100 B	600 s	15 %
HA	50-100 B	10 packets / day	15 %
City lighting	100 B	5 packets / day	5 %
Waste management	10 B	1 packet / hour	37 %
Smart parking	50 B	60 packets / day	28 %

$$- a(h_{rx}) + (44.9 - 6.55 \cdot log_{10}(h_{tx}) \cdot log_{10}(d_{tx-rx})) \quad (38)$$

$$a(h_{rx}) = 0.8 + 1.1 \cdot (log_{10}(fc) - 0.7) \cdot h_{rx} - 1.56 \cdot log_{10}(fc). \quad (39)$$

As discussed in Section IV-C, the number of segments used in the piecewise linear approximation of the RB normalized throughput can be adjusted to achieve arbitrary accuracy in the linearization of the problem's objective function (see (24)). Fig. 3 illustrates the maximum relative error of the approximation for varying numbers of segments and collision probabilities.

As shown, the maximum relative approximation error increases with the allowed collision probability. This behavior arises because higher collision probabilities enable greater maximum traffic intensities on an RB, expanding the interval over which the approximation is applied. Consequently, a larger relative error is expected.

We also analyzed the effect of segment counts (e.g., 1, 2, 4, 8, and 16) on the aggregated normalized throughput given by (3) for target collision probabilities ranging from 10% to 60%. For instance, using the compound traffic model in Table V, the maximum observed coefficient of variation was 0.98%, corresponding to a single channel, a target collision probability of 40%, and a workload of 1200 motes (3 operators with 400 motes each). Based on this analysis, we selected six segments for our setup, as increasing the segment count further did not significantly improve the optimality of the results.

B. Algorithm's Computational Complexity Evaluation

First, we analyze the impact of the number of segments in the piecewise linear approximation of (24) on the execution time. Fig. 4 illustrates the mean execution time as a function of the number of segments considered. The results indicate no significant variation in execution time when the number of segments is adjusted for scenarios involving 300 and 900 EDs. However, as the number of EDs increases, the configuration employing a six-segment approximation demonstrates a lower mean execution time. Therefore, we conclude that selecting a six-segment approximation provides an optimal balance between accuracy and execution time. This approximation is consequently adopted for all subsequent simulations.

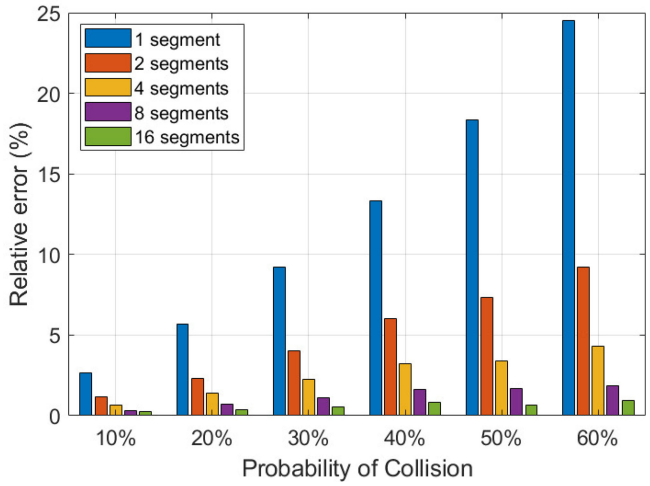


Fig. 3. Maximum relative error between per-RB normalized throughput and its piecewise linear approximation, as a function of the probability of collision and the number of segments.

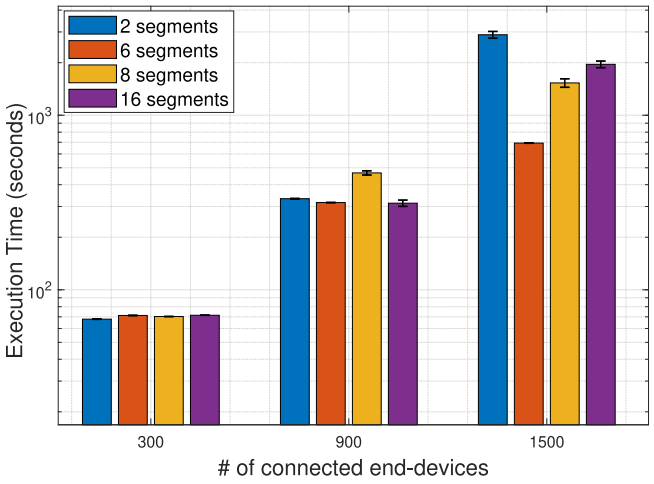


Fig. 4. Mean execution time as a function of the connected EDs and number of segments.

To demonstrate the time and space complexity of this optimization algorithm proposal, several campaigns of simulations have been conducted: for a sweep of the number of total connected EDs in the LoRaWAN network (from 600 to 4500) and for a set of different number of LoRa radio channels (from 1 to 3), 3 runs with random seeds each have been carried out by taking into account the six-segments piecewise approximation. Fig. 5 illustrates the mean execution time (blue color lines) and the number of decision variables needed by the algorithm for its completion (yellow color lines), as a function of two input variables: the total number of connected EDs and the number of LoRa frequency channels under the management

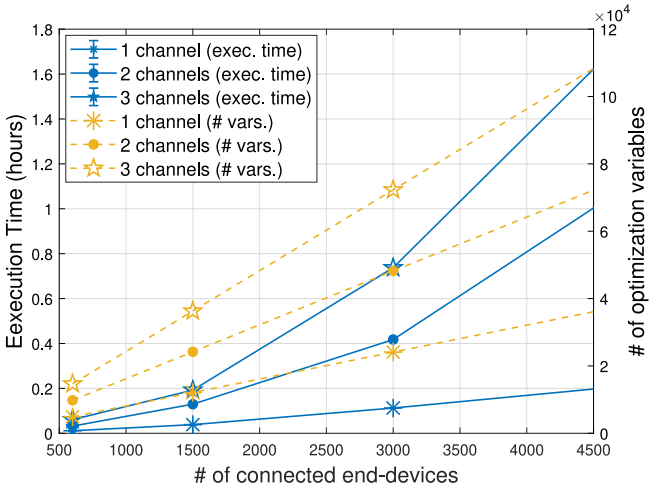


Fig. 5. Total execution time and number of optimization variables as a function of the connected devices.

of the LoRaWAN InP. As it can be seen in the figure, a higher number of connected EDs implies a higher number of optimization variables (following an upward linear trend, which experiences a remarkable growth in the slope of the line when the number of channels increases). When the number of EDs ranges between 500 and 1500, no significant variation in the execution time is observed across configurations with one, two, or three channels. However, as the number of EDs reaches 3000 or more, the execution time for the different channel configurations increases substantially, presenting a clear exponential trend.

C. Algorithm's Performance Evaluation

To illustrate the fulfillment of the problem requirements described in Section IV-A and to analyze the performance of the resource allocation approach, Fig. 6 presents the following performance metrics: the average total demanded traffic from each Network Operator (NO), the average experienced throughput for each NO after the resource allocation process (both metrics expressed in packets/second), and the probability of collision experienced by the InP (expressed on a per unit basis). These metrics are presented as functions of the total number of connected end-devices (600, 1500, 3000, and 4500, corresponding with the total across the three NOs/slices), for a single configured LoRa radio channel. Given that only 6 RBs are considered, corresponding to one LoRa radio channel and a set of 6 SFs, (please, note that an RB comprises a pair of a LoRa radio channel and an SF), it is observed that as the number of EDs and, consequently, the traffic demands on each slice increase, the probability of collision also rises due to the saturation of the resources. In the figure, we can also observe that the average offered throughput by each NO is proportional to their demanded traffic whenever is not possible to align the offered throughput to their demanded traffic, thereby satisfying the second objective of the defined problem (see (4)). In such cases, the difference between the NOs demanded traffic (continuous lines) and offered throughput (dashed lines) is very tiny when there is a low traffic demand (e.g. for NO 1 when 600 EDs are configured, for NO 2 when 4500 EDs are configured or for NO 3 when 600, 1500 and 3000 EDs are configured). For the rest of the cases, where the demanded traffic is higher, there is an average maximum difference between the demanded traffic and the offered throughput in the range of 16%–20%. This is due to the fulfillment of constraint (36) that is configured so that in every RB it should be guaranteed a maximum probability of collision of 20%.

To provide a more general evaluation of the algorithm, we consider a standard LoRaWAN configuration, specifically the default three radio channels at 868.1, 868.3, and 868.5 MHz in the EU863-870 band, as recommended by the LoRaWAN Regional Parameters specification [6]. These channels are the minimum set that a GW must listen to and shall be also implemented in every ED. Fig. 7 represents the same performance metrics of the previously described Fig. 6. In this figure, it can be seen an increment of the demanded traffic load due to the availability of more RBs that allow the InP to accommodate more number of EDs and thus, there is also an increment on the offered throughput in every slice (the NOs are able to course more amount of traffic). In this case, for a number of 4500 EDs, the maximum utilization of the resources is not accomplished so that there is a probability of collision under the maximum 20% defined on the problem requirements.

Additionally, in Fig. 8 it is shown an example of the RB allocation for each of the LoRaWAN NOs in the case of 4500 connected EDs and one radio channel configured. Every different color bar represents the number of EDs of a NO (represented in blue, orange and yellow colors for NO 1, NO 2 and NO 3, respectively) that have been allocated that RB_j (the latter represented on the x-axis as pairs of channels-SF, where RB_1 means channel 1 and SF 12, RB_2 means channel 1 and SF 11 and so on up to the RB_6 representing channel 1 and SF 7). As can be seen in the figure, each RB_j is allocated to one and only one NO showing in this way the isolation in the allocation, and thus meeting constraint (13) presented in Section IV-A. In this case, as there are only 6 RBs and a high number of connected EDs, the allocation has been done by maximizing the offered throughput of each RB until guarantying the maximum collision probability of 20%. As there is not enough capacity and several constraints should be fulfilled, there has been a 32% from the total of the 4500 connected EDs that has not been allocated a RB due to: 1) the transmitted signal of the EDs does not reach the minimum SNR level to be correctly received by the GW; 2) not enough amount of resources; or 3) a guaranteed probability of successful transmissions in every RB should be satisfied.

Fig. 9 represents the allocation of RBs to each NO for a configuration of 4500 connected EDs and 3 radio channels. It is worth emphasizing that, since in this case we have 3 LoRa radio channels with 6 SFs configured each, in total there is a set of 18 RBs to be allocated. As it can be seen, almost all the resources are assigned to the EDs in an isolated way until the maximum probability of collision is reached (a RB is allocated to a unique NO, as expected in scenarios implementing network slicing paradigm). Finally, it should be noted that for certain RBs, a higher number of

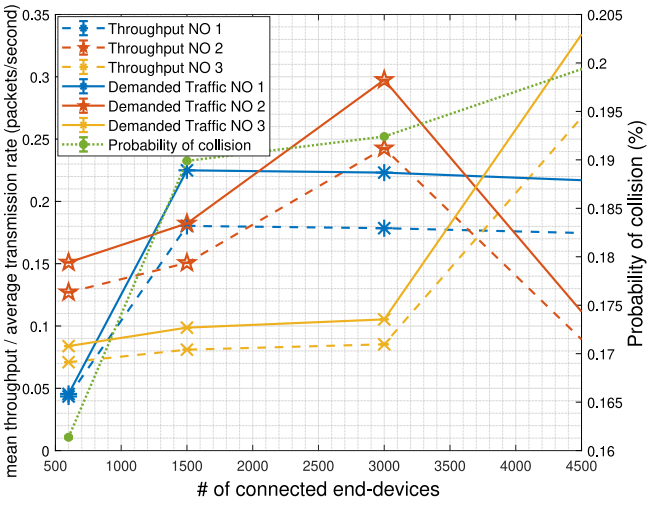


Fig. 6. Total normalized throughput and Probability of collision as a function of the connected devices (1 LoRa radio channel configured).

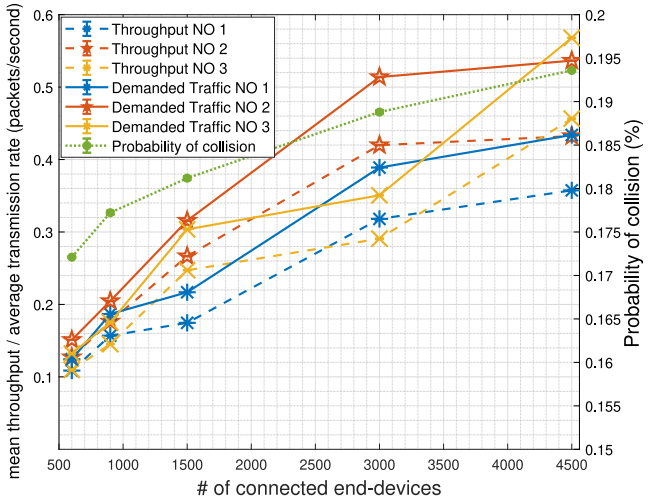


Fig. 7. Total normalized throughput and Probability of collision as a function of the connected devices (3 LoRa radio channels configured).

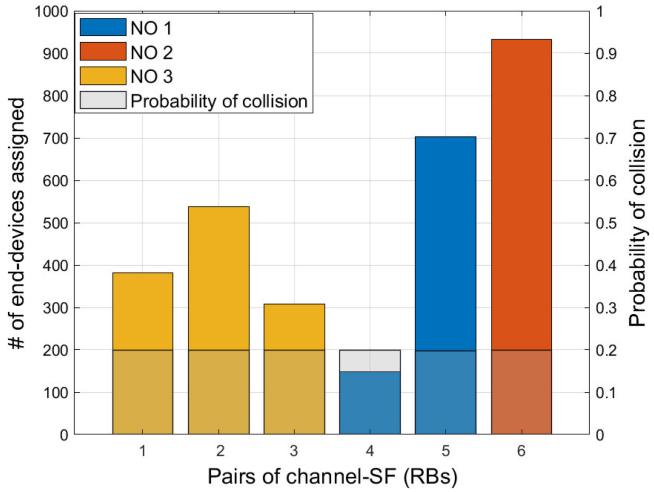


Fig. 8. RBs allocation distribution for a scenario of 4500 connected EDs (1500 EDs per NO) an one radio channel configured.

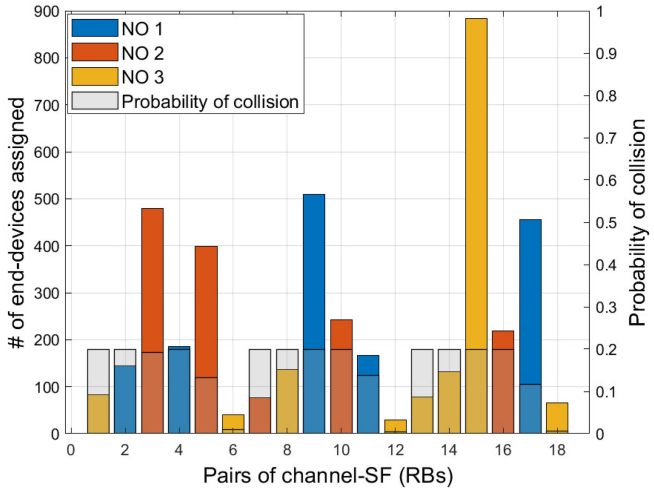


Fig. 9. RBs allocation distribution for a scenario of 4500 connected EDs (1500 EDs per NO) and 3 radio channels configured.

EDs are assigned with respect to others with a lower number of them. This is possible since the traffic model considers IoT applications with distinct packet generation rates, payload sizes, so as the different EDs will be also allocated to a RB that fits well with its QoS requirements (e.g., EDs with a payload size of 100 B should be only assigned to the RBs that correspond to SF 9, SF 8 or SF 7). In this case, only the 2% of the total EDs connected to the network are not assigned an RB.

D. Comparison With Existing Solutions

This section presents a qualitative comparison with existing works. First, it is important to highlight that a direct comparison is neither straightforward nor entirely fair due to the differing assumptions in the scenario and system model of our proposal compared to those in previous studies. However, we have identified the existing solutions that are most in line with our approach. Specifically, we selected the study in [11], which defines three network slices with distinct requirements in terms of delay, PER, Packet Delay Budget (PDB), and priority.

To ensure a fair comparison, we adapted our simulations to match the key system parameters used in that study. Moreover, since it considers a smart city scenario with network slicing, it serves as a relevant benchmark for our evaluation. We replicated the setup from [11], with its main configuration parameters detailed in [11, Table II]. Additionally, to apply our solution to their scenario, we modeled each network slice as an NO in our framework, where motes consume services with the QoS parameters specified in [11, Table I].

For the performance evaluation, we used the PLR as a function of the number of EDs (network load). Fig. 10 presents this comparison with existing works, whose corresponding results are also reported in [11, Fig. 7]. More precisely, we compare our approach against five SF-TP configuration strategies. The static and optimal methods, proposed in [11], serve as baselines. Static assigns fixed values to all devices from a predefined set of SF-TP configurations, ensuring simplicity but lacking adaptability. Dynamic Random (DR) assigns SF and TP randomly, while Dynamic Adaptive (DA) adjusts them based on the highest received power. TOPG

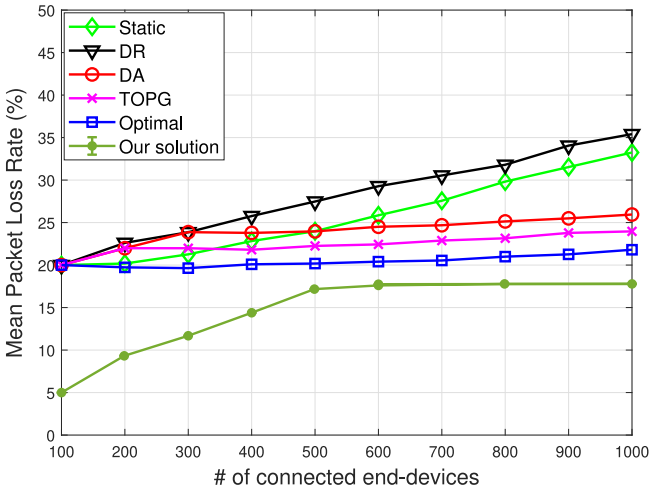


Fig. 10. Comparison of the mean PLR versus the number of connected EDs.

TABLE VI
GINI INDEX AS A FUNCTION OF THE HYPERPARAMETER α

α	mean	std	min	max
0.2	0.14	0.07	0.03	0.26
0.4	0.14	0.07	0.03	0.26
0.6	0.14	0.07	0.03	0.26
0.8	0.14	0.07	0.02	0.33
1.0	0.15	0.08	0.00	0.33

optimizes parameter selection via machine learning and multicriteria decision making, limiting the search space to improve efficiency. The optimal method follows the same principle as TOPG but explores the full search space.

Our solution consistently achieves a lower PLR than all compared approaches, without significant mote discards due to resource shortages. This is primarily due to two factors: first, we employ exact optimization methods—at the cost of higher computational complexity—to determine the optimal allocation of motes to resource blocks, whereas the other solutions rely on nonexact approximations. Second, our optimization framework enforces a strict PLR constraint, ensuring it does not exceed the threshold obtained by the optimal approach at each point. In contrast, the competing solutions treat PLR as an optimization objective rather than a guaranteed constraint. It is important to note that our solution differs fundamentally from the others—it does not configure TP but instead optimizes fairness among operators (slices in these results) and aggregate throughput. Moreover, despite delivering optimal configurations, our approach incorporates regulatory constraints (e.g., duty cycle per ED), which inherently limit resource utilization—an aspect not considered in the alternative solutions.

E. Fairness Evaluation

This section evaluates the fairness of our solution and its impact on the aggregated normalized throughput, which is the other optimization objective. To this end, we conducted a set of simulations varying the number of connected EDs (from 500 to 3000), the number of available LoRa channels (from 1 to 3), and the hyperparameter α (ranging from 0.2 to 1)—see (26). The number of NOs was fixed at two, and we further analyzed the effect of imbalanced traffic demands between them. Specifically, we considered demand ratios of 1:1, 1:2, and 1:3, where 1:1 represents an equal demand distribution across NOs.

We then computed the mean, standard deviation, minimum, and maximum values of the Gini Index, mean aggregated throughput—see (3), and fairness—see (4)—as functions of the hyperparameter α. Specifically, for each value of α, we calculated these statistics across all simulated configurations.

The Gini Index is a widely used metric that evaluates the disparity in resource allocation. A Gini Index of 0 represents perfect fairness, while higher values indicate increasing inequality. By analyzing the Gini Index across different configurations, we assess the impact of fairness constraints on network efficiency. It can be computed as,

$$G.I. = \frac{\sum_{i=1}^{n}\sum_{j=1}^{n}|x_i - x_j|}{2n\sum_{i=1}^{n}x_i}. \tag{40}$$

Table VI presents the obtained statistics of the Gini index values as a function of the hyperparameter α. Our solution maintains a mean Gini index below 0.2 regardless of the α value, suggesting that a reasonable level of fairness is achieved in all cases.

Additionally, our analysis reveals that for α values below 0.6, the Gini index remains largely independent of the number of available channels. However, for $\alpha \geq 0.8$, a significant divergence in the Gini index emerges as the number of channels increases. Furthermore, no clear correlation was observed between the Gini index and the network load. On the other hand, when the traffic demand imbalance between operators increases, the Gini index tends to rise. However, this effect is not particularly pronounced.

Fig. 11 shows the two objective functions: 1) aggregate average throughput—see (3)—(frames per unit of time) and 2) the fairness metric—see (4), as a function of the hyperparameter alpha. As alpha increases, particularly above 0.6 (emphasizing throughput maximization), fairness worsens (moving away from 0). While throughput improves, its increase is not significant, as average statistics are based on multiple channel configurations, where some may reach maximum capacity, limiting further throughput gains.

VI. CONCLUSIONS AND FUTURE WORK

In this work, we propose an offline radio resource allocation framework for multitenancy and NS in LoRa networks. Specifically, we design and solve a MILP using exact optimization methods, implemented with the Gurobi solver. This approach ensures compliance with multiple realistic QoS parameters in a LoRaWAN smart city scenario comprising heterogeneous applications. It also performs efficient resource allocation based on the traffic demands of NOs (tenants/slices) while maximizing overall network throughput.

We evaluate our proposal through simulations involving varying numbers of connected EDs and LoRa radio channels. The results demonstrate consistent performance, with solutions

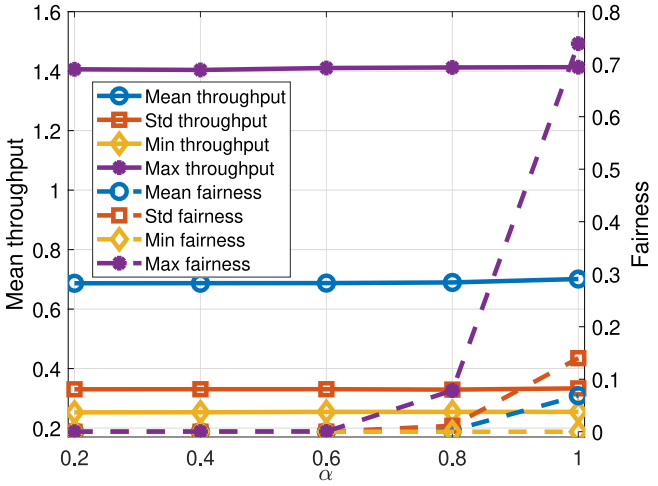


Fig. 11. Objective function outcomes with respect to the hyperparameter α.

obtained in reasonable times (e.g., less than 80 s for 1500 EDs with one channel and under 10 min for three channels). Additionally, the proposed framework satisfies all problem constraints, ensuring fair resource allocation among slices according to their traffic demands, guaranteeing a minimum success probability in each LoRa RB, and maintaining full isolation among resources allocated to different NOs.

This approach provides a practical tool for LoRaWAN InPs to efficiently manage resources across multiple tenants or NOs, ensuring compliance with LoRaWAN standards, QoS metrics, and regulatory constraints.

As future work, an important challenge to address is the development of a radio resource scheduler for LoRaWAN networks that considers the capture effect. While multiple proposals in the literature tackle radio resource planning for LoRaWAN, they often disregard the capture effect—where a packet is not necessarily lost when two nodes transmit simultaneously (collision). Overlooking this phenomenon can lead to a significant underestimation of network performance. In this way, incorporating the capture effect could result in more resource-efficient radio allocation solutions. However, this approach introduces challenges, as the aggregate throughput function of each RB would depend on the number of assigned EDs and their radio conditions. As a result, the problem's complexity would increase substantially, potentially compromising its tractability.

APPENDIX
NP-HARDNESS OF THE PROBLEM

In this annex, we demonstrate the computational complexity (NP-hardness) of our resource allocation problem by constructing a reduction to the Subset Sum Problem. The Subset Sum Problem is a well-known NP-complete problem that involves determining whether a subset of items can be selected such that their weights sum to a given target. By showing that our problem is at least as hard as the Subset Sum Problem, we establish its computational complexity.

The Subset Sum Problem is a classical NP-complete problem for which no polynomial-time algorithm is currently known. It involves determining whether a subset of items from a given set can be selected such that the sum of their weights equals a specified target. This problem is a foundational challenge in combinatorial optimization and is often used as a benchmark for establishing the computational hardness of various problems.

By constructing a reduction that maps an instance of the Subset Sum Problem to an instance of the multitenancy LoRaWAN resource allocation problem with heterogeneous service types, we can demonstrate that our problem is at least as hard as the Subset Sum Problem. Next, the formal proof is included.

Theorem 1: The multitenancy LoRaWAN with heterogeneous service types' resource allocation problem is an NP-hard problem.

Proof: We can prove the theorem by considering a reduced instance version of our problem so that it corresponds to the Subset Sum Problem. To that end, we make the following assumptions.

1. Assume a single LoRaWAN Network Operator (NO) o with a single network slice. This NO manages a set of heterogeneous LoRa EDs, represented as $i \in [1, N_o]$, where N_o is the total number of EDs under the GW coverage. Consequently, objective (4) is no longer used, i.e., $\beta = 0$. Additionally, the isolation constraints (13) among NOs are not applicable.
2. Regarding the physical resources of the LoRaWAN network, we restrict them to a single available channel and a single spreading factor (a single RB), formally denoted as $C = 1$ and $S = 1$, respectively.
3. Suppose there are no duty cycle limitations imposed by regulatory entities.
4. The GW receives a signal level from each ED that exceeds its sensitivity threshold for the specific RB considered.
5. Assume unconfirmed LoRaWAN traffic.

Considering all the above and the definition $\delta_{i,c,s} = U_{i,c} \cdot V_{i,s}$, the original problem (3)–(16) simplifies to

$$\text{maximize}\left\{G_{1,1} \cdot \exp\left(-2G_{1,1}\right)\right\} \tag{41}$$

s.t.

$$G_{s,c} = \sum_{i=1}^{N_o} \delta_{i,1,1} \cdot \lambda_i^{(o)} \cdot T_{i,s}^{(o)} \tag{42}$$

$$\exp\left(-2 \cdot G_{1,1}\right) \geq \left(1 - P_{c,\max}^{(1)}\right). \tag{43}$$

The problem above is equivalent to selecting the EDs such that the aggregated traffic demand $G_{1,1}$ equals a target value G_T. Observe that the target value is given by

$$G_T = \min\left\{-\frac{1}{2} \cdot \ln\left(1 - P_{c,\max}^{(1)}\right), G^*\right\} \tag{44}$$

where G^* is the traffic intensity allocated to the RB that maximizes the normalized throughput function $S_{1,1}$. For the ideal pure ALOHA model, $G^* = 0.5$. Formally, the problem (42)-(43) is equivalent to selecting the EDs ($\delta_{i,1,1} = 1$) whose

aggregated traffic demand comes as close as possible to the target demand

$$\sum_{i=1}^{N_o} \delta_{i,1,1} \cdot \lambda_i^{(o)} \cdot T_{i,s}^{(o)} = G_T. \tag{45}$$

The problem is primarily concerned with selecting items whose weights sum to the target weight, which is known as the Subset Sum Problem, a well-known NP-complete problem [42]. It can be directly observed that the simplified version of our problem corresponds to the Subset Sum Problem. Therefore, we can conclude that our problem is at least as hard as the Subset Sum Problem. ■

ACKNOWLEDGMENT

This work was supported in part by the Spanish Ministry of Science and Innovation funded by MICIU/AEI/10.13039/501100011033, and ERDF/EU under Grant PID2022-137329OB-C43, and in part by the Spanish Ministry for Digital Transformation and Civil Service funded by European Union through the Recovery, Transformation and Resilience Plan–NextGenerationEU under Grant TSI-0630000-2021028/6G-CHRONOS. Funding for open access charge: University of Granada/CBUA.

REFERENCES

[1] "Ericsson mobility report." Ericsson. 2022. [Online]. Available: https://www.ericsson.com/en/reports-and-papers/mobility-report/reports

[2] "3GPP low power wide area technologies," GSMA, London, U.K., White Paper, vol. 11, p. 49, 2018.

[3] *LoRa® and LoRaWAN®: A Technical Overview*, Semtech, Camarillo, CA, USA, Dec. 2019.

[4] J. Ordonez-Lucena, P. Ameigeiras, D. Lopez, J. J. Ramos-Munoz, J. Lorca, and J. Folgueira, "Network slicing for 5G with SDN/NFV: Concepts, architectures, and challenges," *IEEE Commun. Mag.*, vol. 55, no. 5, pp. 80–87, May 2017.

[5] "Short range devices (SRD) operating in the frequency range 25 MHz to 1 000 MHz; part 2: Harmonised standard for access to radio spectrum for non specific radio equipment," ETSI, Sophia Antipolis, France, Rep. 300 220-2, 2018.

[6] *LoRa Alliance®, LoRaWAN® Regional Parameters RP002-1.0.4*, LoRa Alliance®, Fremont, CA, USA, 2022.

[7] *TS001-1.0. 4 LoRaWAN L2 1.0. 4 Specification*, LoRa Alliance, Fremont, CA, USA, Oct. 2020.

[8] S. Dawaliby, A. Bradai, Y. Pousset, and R. Riggio, "Dynamic network slicing for LoRaWAN," in *Proc. 14th Int. Conf. Netw. Service Manag. (CNSM)*, 2018, pp. 134–142.

[9] S. Dawaliby, A. Bradai, and Y. Pousset, "Network slicing optimization in large scale LoRa wide area networks," in *Proc. IEEE Conf. Netw. Softwarization (NetSoft)*, 2019, pp. 72–77.

[10] S. Dawaliby, A. Bradai, and Y. Pousset, "Adaptive dynamic network slicing in LoRa networks," *Future Gener. Comput. Syst.*, vol. 98, pp. 697–707, Sep. 2019.

[11] S. Dawaliby, A. Bradai, and Y. Pousset, "Joint slice-based spreading factor and transmission power optimization in LoRa smart city networks," *Internet Things*, vol. 14, Jun. 2021, Art. no. 100121.

[12] S. Dawaliby, A. Bradai, and Y. Pousset, "Distributed network slicing in large scale IoT based on coalitional multi-game theory," *IEEE Trans. Netw. Service Manag.*, vol. 16, no. 4, pp. 1567–1580, Dec. 2019.

[13] S. Messaoud, A. Bradai, and E. Moulay, "Online GMM clustering and mini-batch gradient descent based optimization for industrial IoT 4.0," *IEEE Trans. Ind. Informat.*, vol. 16, no. 2, pp. 1427–1435, Feb. 2020.

[14] S. Messaoud, A. Bradai, O. B. Ahmed, P. T. A. Quang, M. Atri, and M. S. Hossain, "Deep federated Q-learning-based network slicing for industrial IoT," *IEEE Trans. Ind. Informat.*, vol. 17, no. 8, pp. 5572–5582, Aug. 2021.

[15] E. Ossongo, M. Esseghir, and L. Merghem-Boulahia, "A multi-agent federated reinforcement learning-based optimization of quality of service in various LoRa network slices," *Comput. Commun.*, vol. 213, pp. 320–330, Jan. 2024.

[16] F. Z. Mardi, M. Bagaa, Y. Hadjadj-Aoul, and N. Benamar, "Heuristic-deep Q-network-based network slicing in LoRaWAN," in *Proc. IEEE Int. Conf. Commun.*, 2023, pp. 4731–4736.

[17] F. Z. Mardi, Y. Hadjadj-Aoul, M. Bagaa, and N. Benamar, "Resource allocation for LoRaWAN network slicing: Multi-armed bandit-based approaches," *Internet Things*, vol. 26, Jul. 2024, Art. no. 101195.

[18] G. El Helou, M. Ibrahim, R. El Tawil, and Y. Mohanna, "QoS based IoT applications in LoRa networks using multi-dimensional allocation strategy," *IEEE Access*, vol. 12, pp. 178476–178494, 2024.

[19] T. Bellanger, A. Guitton, R. Stanica, and F. Valois, "Everyone can slice LoRaWAN," in *Proc. 19th Int. Conf. Wireless Mobile Comput., Netw. Commun. (WiMob)*, 2023, pp. 375–380.

[20] H. Fawaz, K. Khawam, S. Lahoud, S. Martin, and M. El Helou, "Cooperation for spreading factor assignment in a multioperator LoRaWAN deployment," *IEEE Internet Things J.*, vol. 8, no. 7, pp. 5544–5557, Apr. 2021.

[21] H. Fawaz, K. Khawam, S. Lahoud, C. Adjih, and S. Martin, "Joint spreading factor and channel assignment in multi-operator LoRaWAN deployments," *Sensors*, vol. 21, no. 1, p. 162, 2020.

[22] D. Bankov, E. Khorov, and A. Lyakhov, "An algorithm to satisfy the QoS requirements in a heterogeneous LoRaWAN network," in *Proc. IEEE Symp. Comput. Commun. (ISCC)*, 2020, pp. 1–6.

[23] A. Tellache, A. Mekrache, A. Bradai, R. Boussaha, and Y. Pousset, "Deep reinforcement learning based resource allocation in dense sliced LoRaWAN networks," in *Proc. IEEE Int. Conf. Consum. Electron. (ICCE)*, 2022, pp. 1–6.

[24] K. Khawam, H. Fawaz, S. Lahoud, O.-A. Maillard, and S. Martin, "A channel selection game for multi-operator LoRaWAN deployments," *Comput. Netw.*, vol. 216, Oct. 2022, Art. no. 109185.

[25] A. Aimi, F. Guillemin, S. Rovedakis, and S. Secci, "Packet delivery ratio guarantees for differentiated LoRaWan services," in *Proc. IEEE Global Commun. Conf.*, 2022, pp. 2014–2019.

[26] A. Aimi, F. Guillemin, S. Rovedakis, and S. Secci, "Traffic control and channel assignment for quality differentiation in dense urban LoRaWANs," in *Proc. 20th Int. Symp. Model. Optim. Mobile, Ad hoc, Wireless Netw. (WiOpt)*, 2022, pp. 153–160.

[27] G. Dandachi and Y. Hadjadj-Aoul, "A frequency-based intelligent slicing in LoRaWAN with admission control aspects," in *Proc. 25th Int. ACM Conf. Model. Anal. Simulat. Wireless Mobile Syst.*, 2022, pp. 189–196.

[28] T. Mai, H. Yao, N. Zhang, W. He, D. Guo, and M. Guizani, "Transfer reinforcement learning aided distributed network slicing optimization in industrial IoT," *IEEE Trans. Ind. Informat.*, vol. 18, no. 6, pp. 4308–4316, Jun. 2022.

[29] "LoRa®, and LoRaWAN®: A technical overview." LoRa Developer Portal. Accessed: Aug. 6, 2024. [Online]. Available: https://lora-developers.semtech.com/documentation/tech-papers-and-guides/lora-and-lorawan/

[30] L. Chinchilla-Romero, J. Prados-Garzon, P. Ameigeiras, P. Muñoz, and J. M. Lopez-Soler, "5G infrastructure network slicing: E2E mean delay model and effectiveness assessment to reduce downtimes in industry 4.0," *Sensors*, vol. 22, no. 1, p. 229, 2022.

[31] T. Cogalan et al., "5G-CLARITY: 5G-advanced private networks integrating 5GNR, WiFi, and LiFi," *IEEE Commun. Mag.*, vol. 60, no. 2, pp. 73–79, Feb. 2022.

[32] "LoRaWAN®." The Things Network. Accessed: Aug. 6, 2024. [Online]. Available: https://www.thethingsnetwork.org/docs/lorawan/

[33] M. Rizzi, P. Ferrari, A. Flammini, and E. Sisinni, "Evaluation of the IoT LoRaWAN solution for distributed measurement applications," *IEEE Trans. Instrum. Meas.*, vol. 66, pp. 3340–3349, 2017.

[34] "137 MHz to 1020 MHz low power long range transceiver," Data Sheet SX1276/77/78/79, Semtech, Camarillo, CA, USA, 2020.

[35] S. Kosunalp, P. D. Mitchell, D. Grace, and T. Clarke, "Experimental study of capture effect for medium access control with ALOHA," *ETRI J.*, vol. 37, no. 2, pp. 359–368, 2015.

[36] D. Bankov, E. Khorov, and A. Lyakhov, "Mathematical model of LoRaWAN channel access with capture effect," in *Proc. IEEE 28th Annu. Int. Symp. Pers., Indoor, Mobile Radio Commun. (PIMRC)*, 2017, pp. 1–5.

[37] S. Liu, "Optimal breakpoint selection method for piecewise linear approximation," 2024, *arXiv:2407.21081*.

[38] A. Sinaeepourfard et al., "Estimating smart city sensors data generation," in *Proc. Mediterranean Ad Hoc Netw. Workshop (Med-Hoc-Net)*, 2016, pp. 1–8.
[39] "Smart cities infographic 2022." 2022. Accessed: Aug. 1, 2024. [Online]. Available: https://resources.lora-alliance.org/smart-cities/smart-cities-infographic-2022
[40] L. Feltrin, C. Buratti, E. Vinciarelli, R. De Bonis, and R. Verdone, "LoRaWAN: Evaluation of link-and system-level performance," *IEEE Internet Things J.*, vol. 5, no. 3, pp. 2249–2258, Jun. 2018.
[41] W. Ingabire, H. Larijani, and R. M. Gibson, "Performance evaluation of propagation models for LoRaWAN in an urban environment," in *Proc. Int. Conf. Electr., Commun., Comput. Eng. (ICECCE)*, 2020, pp. 1–6.
[42] T. H. Cormen, C. E. Leiserson, R. L. Rivest, and C. Stein, *Introduction to Algorithms*. Cambridge, MA, USA: MIT Press, 2022.

Natalia Chinchilla-Romero received the B.Sc. and M.Sc. degrees from the University of Granada (UGR), Granada, Spain, in 2019 and 2021, respectively, where she is currently pursuing the Ph.D. degree with the WiMuNet Laboratory Research Group, Department of Signal Theory, Telematics, and Communications.

Jonathan Prados-Garzon received the B.Sc., M.Sc., and Ph.D. degrees from the University of Granada, Granada, Spain, in 2011, 2012, and 2018, respectively.

He is an Assistant Professor of Telematics Engineering with the University of Granada. He conducted his research primarily with the WiMuNet Laboratory, University of Granada and the MOSA!C Laboratory, Aalto University, Espoo, Finland. His research interests focus on softwarized mobile broadband networks.

Felix Delgado-Ferro received the B.Sc. and M.Sc. degrees in telecommunication engineering from the University of Granada, Granada, Spain, in 2020 and 2022, respectively, where he is currently pursuing the Doctoral degree in telecommunication engineering with the Wireless and Multimedia Networking Laboratory Research Group, Department of Signal Theory, Telematics and Communications.

In 2023, he was a visiting doctoral student with the Simula Research Laboratory, University of Oslo, Oslo, Norway. His current research interests include multipath protocols, heterogeneous networks, and optimization techniques for IoT, 5G, and 6G networks.

Jorge Navarro-Ortiz received the M.Sc.E.E. degree from the University of Malaga, Málaga, Spain, in 2001, and the Ph.D. degree from the University of Granada, Granada, Spain, in 2010.

He worked with the Nokia Networks, Optimi/Ericsson, and Siemens. He started working as an Assistant Professor with the University of Granada, in 2006, where he is currently an Associate Professor with the Department of Signal Theory, Telematics and Communications. His research interests include wireless technologies for the IoT, such as LoRaWAN and 5G/6G.